## Uniform and Simultaneous Orthogonal Functionalization of a Metal-Organic Framework Material

Kanchana P. Samarakoon,<sup>a</sup> Mohammad S. Yazdanparast,<sup>a</sup> Victor W. Day<sup>b</sup> and Tendai Gadzikwa\*<sup>a</sup>

We exploit orthogonal chemical reactivity to generate uniformly multifunctionalized confined spaces. A metal-organic framework (MOF) material that has azide and hydroxyl reactive groups in well-defined locations is independently functionalized to yield a uniformly bifunctionalized material via multiple paths, including via a simultaneous, one-pot reaction.

A long-standing goal of supramolecular chemistry has been the generation of uniform, highly functionalized, confined spaces. Structures of this design are highly sought after as they are anticipated to exhibit the cooperative behaviours of biological structures, specifically those of enzymes.<sup>1–3</sup> But, as the uniform organization of multiple functionalities within confined space is often a herculean synthetic task, few such structures exist despite their desireability.<sup>4–10</sup> Recently however, metal-organic framework (MOF) materials, which possess well-defined pores that can be customized with a wide variety of chemical functionalities via post-synthesis modification,<sup>11,12</sup> have been proposed as a scaffold in which to efficiently generate uniform chemical complexity within confined space.

However, given the objective of developing general routes to a diversity of uniformly multifunctionalized cavities, the exsisting strategies for multiply functionalizing MOFs fall short. With the exclusion of our single report, <sup>13</sup> all other MOF multifunctionalizations have yielded multivariate materials, i.e. non-uniform materials whose cavities are not identical. <sup>14–20</sup> In the sole exception, we introduced a methodology that generates uniformly multifunctionalized MOFs, <sup>13</sup> and established the requirements to undertake such a strategy: i) the framework must be composed of two or more linkers bearing modifiable handles of differing reactivity, ii) the different linkers must be in well-defined positions throughout the framework, and iii) each reaction must be high-yielding, resulting in quantitative conversion (Figure 1A).

We constructed a MOF material, **KSU-1**, composed of two linkers, one bearing amines and the other hydroxyls. The linkers were in well-defined locations throughout the structure and their independent and quantitative functionalization resulted in uniformly multifunctional materials (Figure 1A). While this is an efficient strategy for generating confined spaces that are both complex and uniform, the similar modes of reaction of the amine and hydroxyl reactive groups limit the general use of this particular system. Though the hydroxyls' poorer aptitude for nucleophilic attack allows for independent functionalization,<sup>21</sup> the first reactions are always restricted to those of the –NH<sub>2</sub> groups with the limited range of electrophiles that will not react with the –OH groups. Additionally, the material cannot be modified with moieties that contain better nucleophiles than the hydroxyls. As biological function often involves the action of nucleophilic amines and thiols,<sup>22</sup> this constraint severely diminishes our ability to construct biomimetic materials.

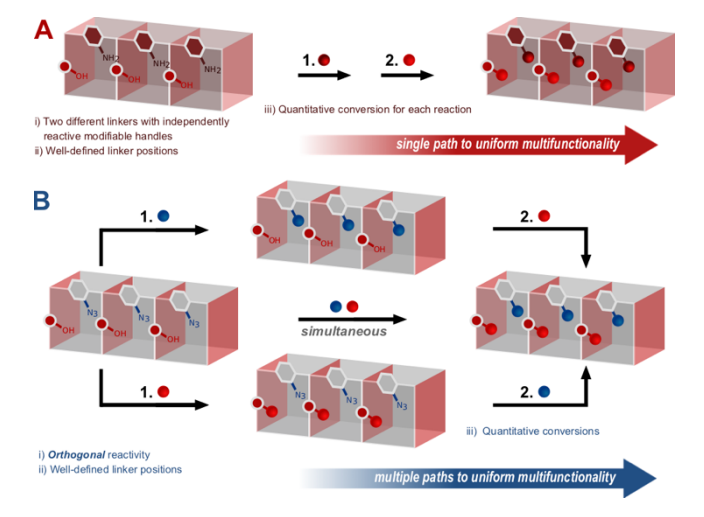


**Fig 1.** A: Functionalization of regularly positioned, independently reactive MOF linkers results in a uniformly multifunctional MOF. B: The use of orthogonally reactive linkers yields a uniformly multifunctional MOF via multiple routes.

To remedy these limitations, we have developed a new system in which the modifiable components have *orthogonal* reactivity, i.e. a system in which the two functional groups only react with their respective reactive partners, with no

possibility of cross reaction.<sup>23,24</sup> While orthogonal MOF functionalization has been previously reported, <sup>18–20</sup> those examples involved multivariate parent MOFs, resulting in nonuniform functionalizations. Our goal in this work is to demonstrate an orthogonal strategy that specifically yields *uniformly* functionalized MOFs. Additionally, we aim to do so via multiple paths, including via a simultaneous reaction (Figure 1B). Multipath reactions allow us to react the –OH first, thus providing greater flexibility in reactant choice for the second reaction. Our approach is to construct a MOF with the same topology as **KSU-1**, but with the amines replaced by azides which can be functionalized via the copper(I) catalyzed azide alkyne cycloaddition (CuAAC) reaction.<sup>25–27</sup> Under CuAAC conditions, only azides react with terminal alkynes, and vice versa, meaning that the reaction is tolerant to the presence of functional groups found in biological systems.<sup>28</sup> Thus, this robust and selective reaction is favorable for use in materials that are already highly functionalized.

We undertook the construction of an orthogonally functionalizable MOF using 2-azido-1,4-benzenediacarboxylic acid (BDC-N<sub>3</sub>) and meso- $\alpha$ , $\beta$ -di(4-pyridyl)glycol (DPG) as our organic linkers (Figure 2A). The linkers were incubated with Zn(NO<sub>3</sub>)<sub>2</sub>·6H<sub>2</sub>O in *N*,*N*-dimethylformamide (DMF) at 60 °C for 24 h, yielding yellow, block-like crystals of **KSU-2**. Single-crystal X-ray diffraction analysis revealed the crystals to be those of a mixed-linker MOF material (Figure 3B-C). The BDC-N<sub>3</sub> linkers are connected by Zn-paddlewheel secondary building units (SBUs) in the ab-plane, forming 2D Kagometype sheets that are pillared by DPG linkers along the *c*-axis. The triangular and hexagonal channels running down the *c*-axis are 1 nm and 1.7 nm across, respectively. The purity of bulk phases of **KSU-2** was determined by powder X-ray diffraction (PXRD), Figure S1, and supported by proton nuclear magnetic resonance ( $^1$ H-NMR) spectroscopy of the material digested in a solution of deuterosulfuric acid (D<sub>2</sub>SO<sub>4</sub>) in deuterated dimethylsulfoxide (DMSO-d<sub>6</sub>) (Figures 3B and S2). The material retains very little porosity under evacuation, as determined by N<sub>2</sub> adsorption (Figure S3), however, thermogravimetric analysis (TGA) of **KSU-2** (Figure S4) indicates that the material has substantial solvent-accessible volume. The MOF loses ~45 % of its weight as DMF upon heating, supporting our expectation that **KSU-2** would have ample room for multifunctionalization.

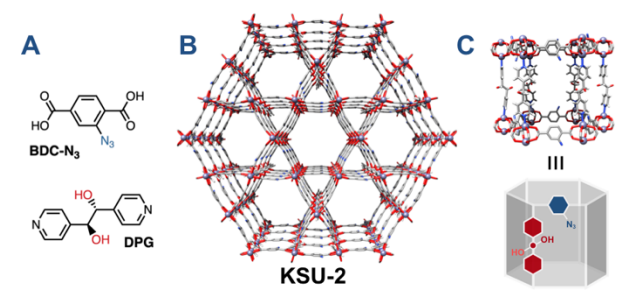
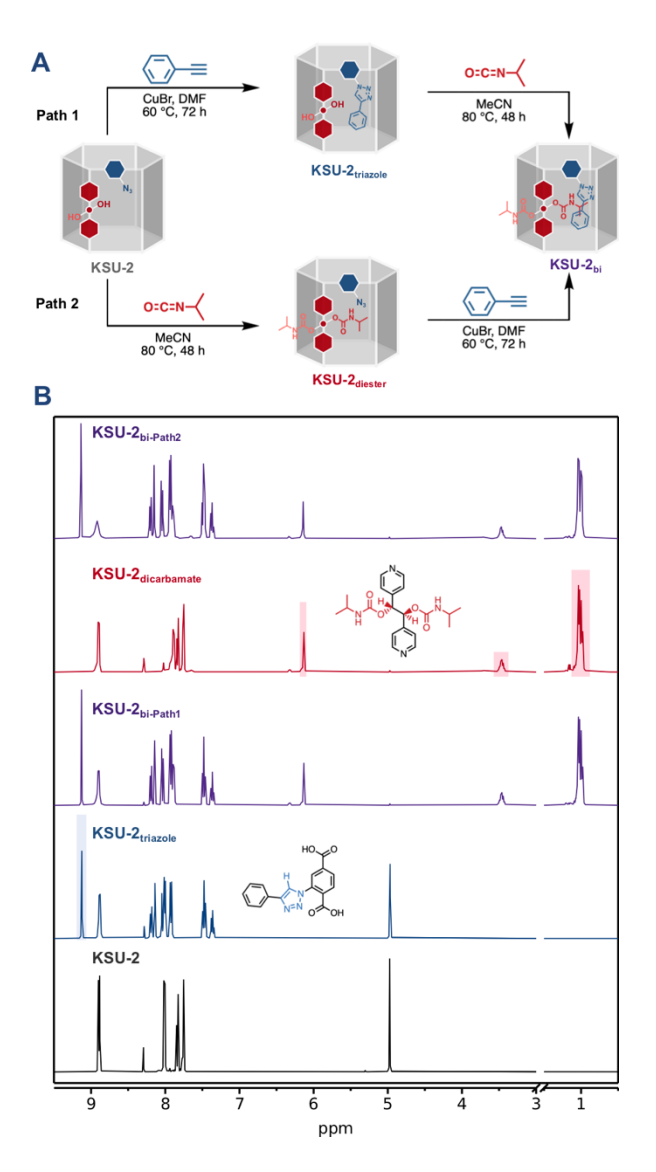


Fig 2. A: Orthogonally reactive linkers. B: KSU-2 viewed down the c-axis. C: Network unit of KSU-2 and its schematic representation.

For the multifunctionalization of **KSU-2**, we elected to react the azides with phenylacetylene, and the hydroxyls with isopropyl isocyanate (Figure 3A). Following a modified literature procedure, <sup>29</sup> **KSU-2** was incubated in a DMF solution of phenylacetylene and CuBr catalyst under a nitrogen atmosphere at 60 °C, with constant agitation. Monitoring the reaction product by observing the disappearance of the azide stretching frequency peak of **KSU-2** in the Fourier-transform infrared (FTIR) spectrum (Figure S5) revealed that the reaction was complete after 72 h. Additionally, the <sup>1</sup>H-NMR spectrum of the digested material had peaks corresponding to protons of both DPG and the clicked BDC-N<sub>3</sub> product, BDC<sub>triazole</sub>, <sup>30</sup> and none for BDC-N<sub>3</sub> (Figure 3B). High resolution electrospray ionization mass spectrometry (ESI-MS) of a solution of the clicked MOF, **KSU-2**<sub>triazole</sub>, disassembled in a solution of 1,4-diazabicyclo[2.2. 2]octane (DABCO) in DMSO gave a positive mode spectrum with mass signals corresponding to [BDC<sub>triazole</sub>-H<sup>+</sup>] and [DPG+H<sup>+</sup>] (Figure S6), confirming the quantitative and selective grafting of the alkyne to the azide. Although N<sub>2</sub> adsorption revealed continued minimal porosity following evacuation (Figure S3), confirmation of crystallinity by PXRD (Figure S1) and retention of significant solvent-accessible volume by TGA (~30 weight % solvent, Figure S4), encouraged us to proceed with the functionalization of the DPG ligand of **KSU-2**<sub>triazole</sub>.



**Fig 3.** A: Schematic representation of the multipath, orthogonal functionalization of **KSU-2** with phenyl acetylene and isopropyl isocyanate. B: <sup>1</sup>H-NMR spectra of **KSU-2**<sub>triazole</sub>, **KSU-2**<sub>bi-Path1</sub>, **KSU-2**<sub>dicarbamate</sub>, and **KSU-2**<sub>bi-Path2</sub> digested in a solution of D<sub>2</sub>SO<sub>4</sub> in DMSO-*d*<sub>6</sub>. C: FT-IR spectra of each material in the functionalization sequence, focusing on the triazole peak at 2117 cm<sup>-1</sup>. B: Simultaneous, independent functionalization of **KSU-2** with phenyl acetylene and isopropyl isocyanate.

Isocyanates have been used before to functionalize amine-bearing MOFs, \$^{15,31,32}\$ and we selected the same electrophile to react with the hydroxyls of DPG to produce DPG<sub>dicarbamate</sub>. Previously we reacted DPG with a cyclic anhydride resulting in products with ester linkages. \$^{13}\$ The advantage of the current reaction is that the carbamate linkage has higher chemical stability, \$^{33}\$ which simplifies characterization of the products. Following a modified procedure, \$^{34}\$ we immersed KSU-2<sub>triazole</sub> in a solution of isopropyl isocyanate in acetonitrile, with continuous agitation at 80 °C for 48 h to produce the bifunctionalized product, KSU-2<sub>bi-Path1</sub>. The complete shift of the protons alpha to the glycol in the \$^{1}\$H-NMR spectrum of KSU-2<sub>bi-Path1</sub> indicated the quantitative conversion of the hydroxyls to carbamates (Figure 3B). The covalent grafting of the isocyanate to the hydroxyls was confirmed by disassembling KSU-2<sub>bi-Path1</sub> in a solution of DABCO in DMSO-\$d\_6\$. High resolution electrospray ionization mass spectrometry (ESI-MS) of the solution gave a positive mode spectrum that pseudo molecular ion signals corresponding to [BDC<sub>triazole</sub>-H<sup>+</sup>] and [DPG<sub>dicarbamate</sub>+H<sup>+</sup>]. The most significant peaks corresponded to the McLafferty rearrangement fragment [DPG<sub>dicarbamate</sub>-CO<sub>2</sub>-<sup>i</sup>PrNH<sub>2</sub>+H<sup>+</sup>], \$^{35,36} as well as that fragment ion minus neutral \$^{i}PrNCO.\$^{37}\$ The PXRD pattern (Figure S1) indicates that the material retains its crystallinity and the TGA confirms that an appreciable amount of solvent-accessible volume remains, as indicated by the ~20 % weight loss of DMF (Figure S4).

Having established the success of independent binary functionalization to produce **KSU-2**<sub>bi-Path1</sub> via Path 1, we attempted to obtain the same product via Path 2 (Figure 3A). Using previous reaction protocols (vide supra) we first reacted **KSU-2** with isopropyl isocyanate to produce **KSU-2**<sub>dicarbamate</sub>. The <sup>1</sup>H-NMR spectrum of **KSU-2**<sub>dicarbamate</sub> digested

in acid confirmed the covalent attachment of isocyanate to DPG (Figure 3B), as did the ESI-MS of the DABCO-digested solution (Figure S6). Additionally, a peak corresponding to the azide stretch of BDC-N<sub>3</sub> was still present in the FTIR (Figure S5). An interesting result was that, following the reaction with isopropyl isocyanate, the material appeared to be slightly more stable of evacuation, based on the N<sub>2</sub> adsorption experiments (Figure S3). However, the PXRD pattern of the activated material did not appear to be any more crystalline than the other materials (Figure S1B). The CuAAC reaction of **KSU-2**<sub>dicarbamate</sub> with phenylacetylene produced the bifunctionalized material, **KSU-2**<sub>bi-Path2</sub>, with the same characteristics as **KSU-2**<sub>bi-Path1</sub>: the azide peak in the FTIR had disappeared, the  $^1$ H-NMR had peaks corresponding to BDC<sub>triazole</sub>, and the ESI-MS had signals for [DPG<sub>dicarbamate</sub>+H<sup>+</sup>] and [BDC<sub>triazole</sub>+H<sup>+</sup>] (Figure S6).

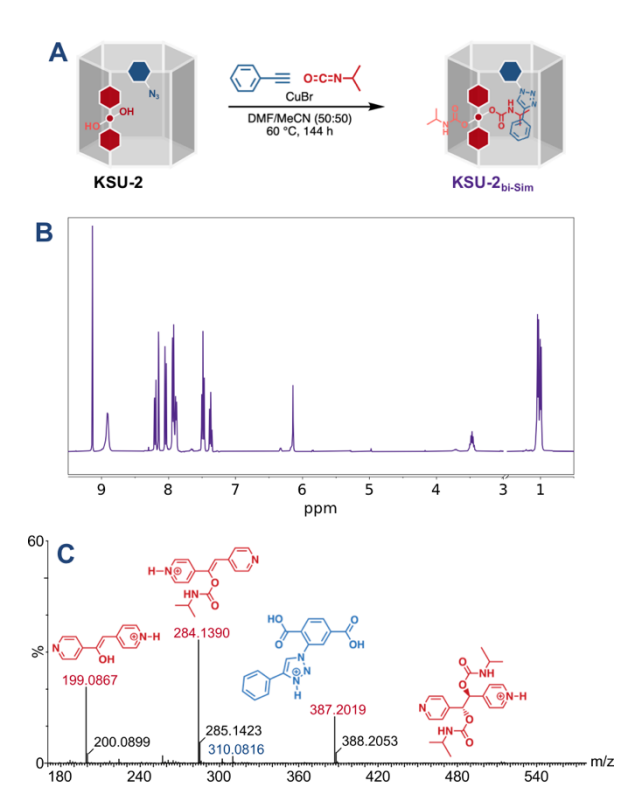


**Fig 4.** A: Schematic representation of the simultaneous, orthogonal functionalization of KSU-2 with phenyl acetylene and isopropyl isocyanate. B: 1H-NMR spectra of the simultaneous reaction product, KSU-2bi-Sim digested in a solution of D2SO4 in DMSO-d6. C: High resolution, positive mode, mass spectrum of KSU-2bi-Sim digested in a DMSO solution of DABCO. The peaks correspond to [DPGdicarbamate+H+], along with its McLafferty rearrangement fragments, and [BDCtriazole-H+].

To demonstrate an additional advantage of orthogonal reactivity, we sought to obtain the final product by performing the functionalizations at the same time (Figure 4A). We took **KSU-2** and performed the CuAAC reaction with phenylacetylene in the presence of isopropyl isocyanate, using a 1:1 mixture of DMF:MeCN. Characterization of the final product confirmed the success of the one pot, independent reaction. The <sup>1</sup>H-NMR and ESI-MS (Figure 4B-C), as well as FTIR (Figure S5) were all consistent with the bifunctional material **KSU-2**<sub>bi-Sim</sub>.

In conclusion, we have improved the utility of our recently developed method for the uniform binary functionalization of MOFs. The orthogonal reactivity offers more flexibility in how the functionalizations can be undertaken. Of particular interest is that the azide group of **KSU-2** is near bioorthogonal, meaning that the MOF can be functionalized with functionalities commonly found in biology without the need for sterically demanding protecting groups that may require harsh conditions to remove. Thus, this development propels us further along in our quest to develop a general platform for generating confined spaces that are uniformly decorated with multiple functional groups, i.e. spaces that can imitate the cooperative functionality of those found in natural systems. Future work in this area will involve the incorporation of catalytic moieties to demonstrate cooperative catalysis in confined spaces.

This study was supported by National Science Foundation grant CHE-1800517, and MRI grants for instruments used in this study (CHE-0923449 to the University of Kansas for the X-ray diffractometer and software and CHE-1826982 to Kansas State University for the NMR spectrometer). The authors acknowledge the Aakeröy Lab at KState for use of their TGA.

## References

- 1 M. Raynal, P. Ballester, A. Vidal-Ferran and P. W. N. M. van Leeuwen, Chem. Soc. Rev., 2014, 43, 1734–1787.
- S. Zarra, D. M. Wood, D. A. Roberts and J. R. Nitschke, Chem. Soc. Rev., 2014, 44, 419–432.
- 3 E. Kuah, S. Toh, J. Yee, Q. Ma and Z. Gao, Chem. Eur. J., 2016, 22, 8404–8430.
- 4 P. Mattei and F. Diederich, *Helv. Chim. Acta*, 1997, **80**, 1555–1588.
- 5 I. Čorić and B. List, *Nature*, 2012, **483**, 315–319.
- 6 L. J. Jongkind, X. Caumes, A. P. T. Hartendorp and J. N. H. Reek, *Acc. Chem. Res.*, 2018, **51**, 2115–2128.
- 7 J. Yang, B. Chatelet, D. Hérault, J.-P. Dutasta and A. Martinez, Eur. J. Org. Chem., 2018, 2018, 5618–5628.
- S. Yuan, Y.-P. Chen, J.-S. Qin, W. Lu, L. Zou, Q. Zhang, X. Wang, X. Sun and H.-C. Zhou, J. Am. Chem. Soc., 2016, 138, 8912–8919.
- 9 L. Liu, T.-Y. Zhou and S. G. Telfer, J. Am. Chem. Soc., 2017, 139, 13936–13943.
- 10 T.-Y. Zhou, B. Auer, S. J. Lee and S. G. Telfer, J. Am. Chem. Soc., 2019, 141, 1577–1582.
- 11 S. M. Cohen, Chem. Rev., 2012, 112, 970-1000.
- 12 S. M. Cohen, J. Am. Chem. Soc., 2017, 139, 2855–2863.
- 13 K. P. Samarakoon, C. S. Satterfield, M. C. McCoy, D. A. Pivaral-Urbina, T. Islamoglu, V. W. Day and T. Gadzikwa, *Inorg. Chem.*, 2019, **58**, 8906–8909.
- 14 Z. Wang and S. M. Cohen, Angew. Chem. Int. Ed., 2008, 47, 4699-4702.
- 15 S. J. Garibay, Z. Wang, K. K. Tanabe and S. M. Cohen, *Inorg. Chem.*, 2009, **48**, 7341–7349.
- 16 L. L. Keenan, H. A. Hamzah, M. F. Mahon, M. R. Warren and A. D. Burrows, CrystEngComm, 2016, 18, 5710–5717.
- 17 A. M. Fracaroli, P. Siman, D. A. Nagib, M. Suzuki, H. Furukawa, F. D. Toste and O. M. Yaghi, *J. Am. Chem. Soc.*, 2016, 138, 8352–8355.
- 18 M. Kim, J. F. Cahill, K. A. Prather and S. M. Cohen, Chem. Commun., 2011, 47, 7629–7631.
- 19 C. Liu, T.-Y. Luo, E. S. Feura, C. Zhang and N. L. Rosi, *J. Am. Chem. Soc.*, 2015, **137**, 10508–10511.
- 20 U. Fluch, B. D. McCarthy and S. Ott, *Dalton Trans.*, 2018, **48**, 45–49.
- 21 H. Mayr and A. R. Ofial, J. Phys. Org. Chem., 2008, 21, 584-595.
- 22 E. M. Sletten and C. R. Bertozzi, Acc. Chem. Res., 2011, 44, 666-676.
- 23 M. Malkoch, R. J. Thibault, E. Drockenmuller, M. Messerschmidt, B. Voit, T. P. Russell and C. J. Hawker, *J. Am. Chem. Soc.*, 2005, **127**, 14942–14949.
- 24 C.-H. Wong and S. C. Zimmerman, Chem. Commun., 2013, 49, 1679–1695.
- 25 C. W. Tornøe, C. Christensen and M. Meldal, J. Org. Chem., 2002, 67, 3057–3064.
- 26 V. V. Rostovtsev, L. G. Green, V. V. Fokin and K. B. Sharpless, *Angew. Chem. Int. Ed.*, 2002, **41**, 2596–2599.
- 27 J. E. Hein and V. V. Fokin, Chem. Soc. Rev., 2010, 39, 1302-1315.
- 28 E. M. Sletten and C. R. Bertozzi, Angew. Chem. Int. Ed., 2009, 48, 6974-6998.
- 29 X.-C. Yi, F.-G. Xi, Y. Qi and E.-Q. Gao, RSC Adv., 2014, 5, 893-900.
- 30 M. Savonnet, D. Bazer-Bachi, N. Bats, J. Perez-Pellitero, E. Jeanneau, V. Lecocq, C. Pinel and D. Farrusseng, *J. Am. Chem. Soc.*, 2010, **132**, 4518–4519.
- 31 E. Dugan, Z. Wang, M. Okamura, A. Medina and S. M. Cohen, Chem. Commun., 2008, 3366-3368.
- 32 S. Bernt, V. Guillerm, C. Serre and N. Stock, Chem. Commun., 2011, 47, 2838-2840.
- 33 A. K. Ghosh and M. Brindisi, *J. Med. Chem.*, 2015, **58**, 2895–2940.
- 34 X.-W. Dong, T. Liu, Y.-Z. Hu, X.-Y. Liu and C.-M. Che, Chem. Commun., 2013, 49, 7681–7683.
- 35 F. W. McLafferty, Anal. Chem., 1959, 31, 82-87.
- 36 C. Wolf, C. N. Villalobos, P. G. Cummings, S. Kennedy-Gabb, M. A. Olsen and G. Trescher, *J. Am. Soc. Mass Spectrom.*, 2005, **16**, 553–564.
- 37 Y. Zhou, J. Guan, W. Gao, S. Lv and M. Ge, *Molecules*, 2018, 23, 2496.